RELICT SHORELINES AND ICE FLOW PATTERNS OF THE NORTHERN PUGET LOWLAND FROM LIDAR DATA AND DIGITAL TERRAIN MODELLING

BY
DORI J. KOVANEN AND OLAV SLAYMAKER

Department of Geography, University of British Columbia, Vancouver, British Columbia

Kovanen, D.J. and Slaymaker, O., 2004: Relict shorelines and ice flow patterns of the northern Puget Lowland from lidar data and digital terrain modelling. *Geogr. Ann.*, 86 A (4): 385–400.

ABSTRACT. Airborne lidar data from the northern Puget Lowland provide information on the spatial variability and amplitude of raised postglacial shorelines, marine deltaic features and glaciomarine sediments deposited between approximately *c.* 12 920 and 11 050 ^{14}C yr BP (15 960–12 364 cal yr BP). Relict shorelines preserved in embayments on Whidbey and Camano islands (between 47°54'N and 48°24'N) are found up to an altitude of *c.* 90 m and record glacio-isostatic movements attributed to postglacial rebound. The tilt of the regional minimum highstand sea level surface to the north of 0.80 m km^{-1}, with local variability from 0.25 m km^{-1} to 0.77 m km^{-1}, is consistent with previous studies (Thorson 1989; Dethier *et al.* 1995). The local variability is related to the uncertainty in the depth of the water column above these features at the time of deposition and probable tectonic deformation. The information generated by these lidar data is most valuable in posing new research questions, generating alternative research hypotheses to those already formulated in the northern Puget Lowland.

Key words: sea level change, relict shorelines, lidar data, digital terrain modelling, postglacial uplift, Puget Lowland

Introduction

The expansion of glaciers during the late Pleistocene led to isostatic depression of the Puget Sound basin (Fig. 1). In the northern Puget Lowland, Whidbey and Camano islands were buried under 1.4–1.2 km of ice when ice reached its maximum extent (Easterbrook 1979; Thorson 1989; Porter and Swanson 1998).). At that time sea levels stood about 130–120 m lower than today (Lambeck *et al.* 2002). At the end of the last glaciation rapid ice melting resulted in sea level rise and rapid uplift of the area. The altitude of the upper marine limit provides an estimate of paleo-sea levels and here is a function of the ice load history, mantle rheological properties, and coastal response to changes in sea level. On Whidbey and Camano islands, indicators of sea level change are preserved along a complex coastline of bays and peninsulas (Figs. 1, 2). The marine limit is known from thick sequences of ice-contact outwash, glaciomarine, deltaic and shoreline sediments that were deposited up to *c.* 90 m above the present sea level shortly after *c.* 13 000 ^{14}C yr BP (Easterbrook 1963, 1992, 1994; 2003; Pessl *et al.* 1989; Dethier *et al.* 1995). The minimum local glacio-isostatic depression is about 190 m considering that eustatic sea level was about 100 m lower at that time.

The challenges of a sea level change study in this region include the identification of shoreline features in areas of relatively dense vegetation cover and establishing reliable means for the correlation of these scattered shorelines and surfaces. This is further complicated by the presence of active tectonic structures (e.g. Thorson 1996). The fault zones in the study area collectively represent a complex, broadly distributed, transpressional deformation zone, which extends westward from the Cascades Range foothills across the eastern Strait of Juan de Fuca.

The aim of this paper is to show how digital terrain modelling using high-resolution lidar data of Whidbey and Camano islands, combined with an understanding of process-form relations can be used to provide information on the uplift pattern in the northern Puget Lowland. Our approach is to provide height information from lidar data of sea level indicators along a transect oriented N–S, roughly parallel to the direction of ice movement. We then compare these results with those of Thorson (1989) and Dethier *et al.* (1995) who calculated average uplift gradients ranging from 0.6 m km^{-1} to 1.15 m km^{-1}. These projections extend the work of Thorson northward, from the transition of sea level indicators from short-lived proglacial lakes into glaciomarine and marine environments in a similar manner to that

Fig. 1. Map of northwestern Washington showing extent and thickness (m) of the Puget Lobe during the Vashon maximum of the last glaciation (Fraser). Ice-surface contours reproduced from Porter and Swanson (1998). The transects A, B, and C are from Dethier *et al.*. (1995), this study, and Thorson (1989), respectively. Refer to Fig. 9 for details

of Dethier *et al* (1995). In addition, we present geomorphic information that relates to the ice flow directions of these islands to provide information of the melting history of ice in this area.

Study area – regional setting

The Puget Lowland lies in a broad forearc depression between the Cascadia subduction zone where the Juan de Fuca plate descends under North America, and the volcanic arc. The Puget basin is situated between the Olympic Mountains to the west and Cascade Range to the east (Fig. 1). During the last glaciation (Fraser Glaciation; Armstrong *et al.* 1965), two major lobes of ice emerged from the Coast Mountains and Cascade Range of British Columbia and extended toward the continental shelf via the Strait of Juan de Fuca and into the Puget Lowland *c.* 18 000–10 000 ^{14}C yr BP. The Juan de Fuca Lobe reached its maximum extent on the continental shelf shortly before 14 460 ± 200 ^{14}C yr BP (Heusser 1973) and the Puget Lobe reached its maximum extent about 14 500 ^{14}C yr BP (Porter and Swanson 1998).

Glacial retreat began shortly after the glacial maximum and reached northern Whidbey Island by about 12 850 ± 60 ^{14}C yr BP (15 868–14 438; Dethier *et al.* 1995). Ten radiocarbon dates from bivalves in ice-proximal environments (Easterbrook 1992; Dethier *et al.* 1995; Kelsey *et al.* 2004; Swanson and Caffee 2001) constrain the time of marine inundation and isostatic uplift. The marine reservoir corrected age is between *c.* 12 920 and 11 050 ^{14}C yr BP (15 960–12 364 cal yr BP). Offshore, a number of sediment cores within the Juan de Fuca Strait indicate deposition of glaciomarine sediment during waning glacial influence and rising sea level between a marine reservoir corrected age of 12 890 ± 50 and 9920 ± 50 ^{14}C yr BP (Hewitt and Mosher 2001).

A problem related to the timing of sea level changes in this area is the radiocarbon age of marine shells from marine and glaciomarine deposits. Many of the ages were not adjusted (Dethier *et al.* 1995) for the effects of ^{14}C-deficient oceanic water or assumed low values for the oceanic reservoir correction which have large uncertainties associated with the stratigraphic context of the samples and measured laboratory precision of the ages (Anundsen *et al.* 1994; Swanson and Caffee 2001). In this paper, marine shells were corrected using a total marine reservoir value of –800 ± 25 years (Robinson and Thompson 1981). This may be conservative as a mean marine reservoir age of –1100 ± 100 years was derived in the Fraser Lowland, 70 km to the northeast (Kovanen and Easterbrook 2002a) and this raises concern regarding the spatial distribution and temporal pattern of sea level and paleoenvironmental changes in this region.

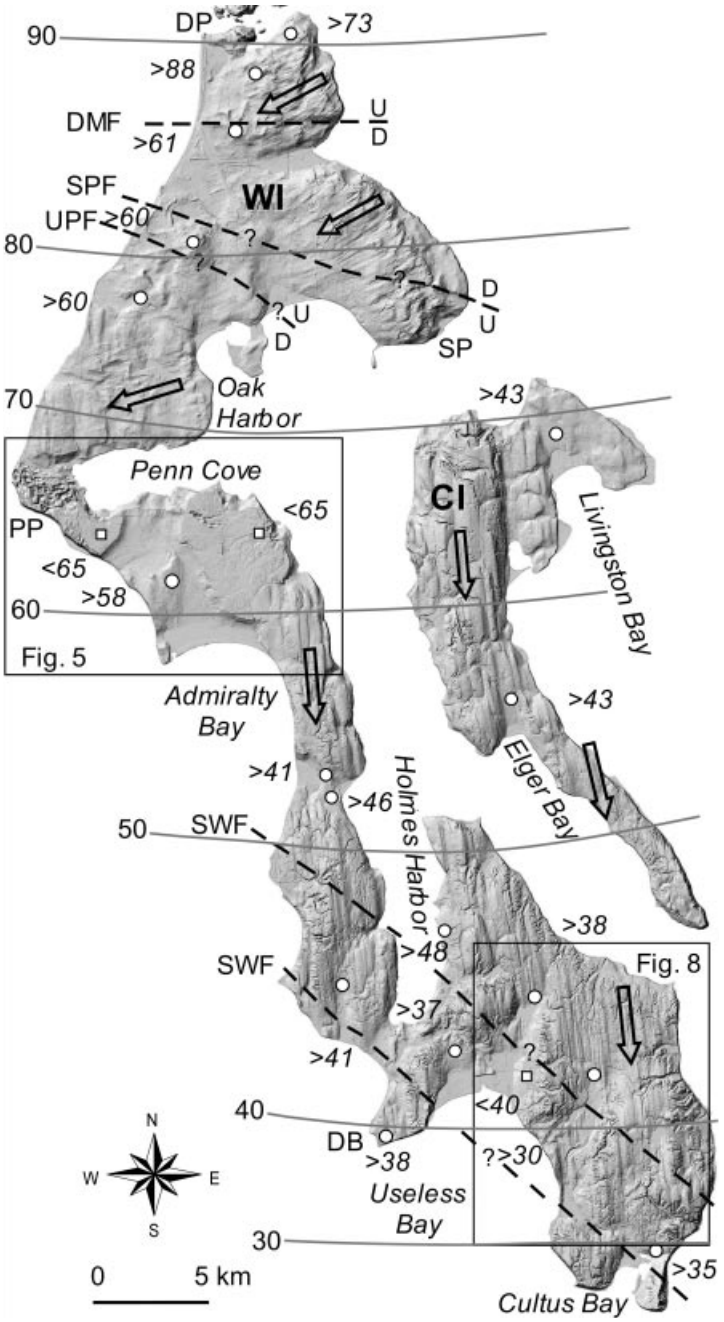

Fig. 2. Shaded digital topographic model of Whidbey and Camano islands from lidar data. O, location of raised shoreline and the corresponding number is the minimum altitude of the marine limit (m); □, raised deltas. Dashed lines are Quaternary fault zones (from Johnson *et al.* 1996, 2002). Contours are the altitude of the marine limit taken from Dethier *et al.* (1995). Arrows indicate the inferred ice-flow direction. WI – Whidbey Island; CI – Camano Island; DP – Deception Pass; SP – Strawberry Point; PP – Partridge Point; DB – Double Bluff; DMF – Devils Mountain Fault; SPF – Strawberry Point Fault; UPF – Utsalady Point Fault; SWF – Southern Whidbey Island Fault. Whidbey Island is *c.* 60 km long and 16–2 km wide, with an altitude up to *c.* 150 m

Previously, the local upper limit of the marine highstand was established by the altitude of glaciomarine deposits in coastal exposures, small-scale road-side exposures, gravel pits (Easterbrook 1969, 1992, 2003; Domack 1983, 1984; Pessl *et al.* 1989; Dethier *et al.* 1995), marine terraces, topsets of marine delta, spillways associated with proglacial lakes and shorelines features (Thorson 1989), and the change from marine to freshwater sedimentation in lake basins (Anundsen *et al.* 1994; Kelsey

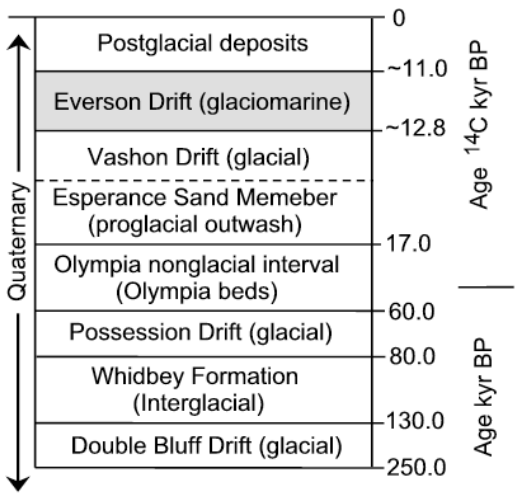

Fig. 3. Stratigraphy and age of unlithified Quaternary geologic units occurring in the northern Puget Lowland.

et al. 2004). Other researchers (Blunt *et al.* 1987; Berger and Easterbrook 1993; Easterbrook 1963, 1992, 1994; Porter and Swanson 1998) have provided numerical constraints for Pleistocene deposits and described the Quaternary unlithified geologic units, three of which are exposed in our study area (Fig. 3). They typically consist of till, outwash, and glaciomarine deposits. Mapping of surficial materials in our study area was completed at the 1:100 000-scale (Pessl *et al.* 1989). Recently, Haugerud *et al.* (2003) and Kovanen (2003) used lidar data to help visualize the topography of the area. Other work has explored various properties of the mantle through modelling tilting of paleoshorelines (James *et al.* 2002).

The local tectonic component in the uplift of this area may have caused local disturbances in surficial deposits. Active tectonic structures are known as the Devils Mountain, Strawberry Point, Utsalady Point and southern Whidbey fault zones and represents boundaries between major crustal blocks (e.g. Johnson *et al.* 1996, 2002). Individual deformation zones are up to *c.* 2 km wide when they cross northern Whidbey Island (Fig. 2) and other possible segment boundaries may be present. Southern Whidbey Island may have experienced 2–1 m of abrupt uplift associated with an earthquake between *c.* 3200–2800 cal yr BP (Kelsey *et al.* 2004). Hence, significant differences may exist across these zones. Our height information may help discriminate the vertical deformation, especially if features exhibit anomalous altitude information relative to the local trend of the uplift pattern.

Data sources and methods

Lidar data

Lidar is short for Light Detection And Ranging, which is also known as an airborne laser swath terrain mapping system. This system is fixed to a winged aircraft or helicopter and uses laser pulses in much the same way that sonar uses sound or radar uses radio waves to measure the round-trip travel of short-duration pulses. The system is linked to a differential Global Positioning System (GPS) for aircraft location/orientation and discrete measurements. The data is initially reduced from XYZ coordinates for each discrete return point and then the reflective surface of the forest canopy is separated from the ground by geometric filtering to generate accurate high-resolution digital terrain images. The vertical and horizontal accuracy of the data is dependent on the type of lidar system used (discrete return or full waveform systems), its configuration, orientation errors associated with GPS, and the propagation of errors through filtering of the data. The reader is referred to Baltsavias (1999), and Wehr and Lohr (1999) for details of lidar theory.

The lidar data used in this study were provided by the **Puget Sound Lidar Consortium** (**PSLC** 2002) and Puget Sound Regional Council. The original contract for the lidar surveys was for researchers and other agencies to uncover topographic expressions of fault traces for seismic hazard studies in the Seattle and surrounding Puget Lowland area (Haugerud *et al.* 2003). The contracted measurement density was 1 pulse/m^2 or 10 000–80 000 laser pulses/s. The resulting topography has a resolution of 2–1 m, with a vertical accuracy on the order of 15 cm. These data were transformed into 6×6 ft (or 1.8×1.8 m) grids and then used to construct a Triangulated Irregular Network (TIN) for visualization with a few modifications to the original data points (PSLC 2002). The data were supplied in quarter-township tiles (4.8×4.8 km) and then we merged them for seamless representation of the topography. We have not fully assessed the accuracy of the lidar data, although it appears that the supplied data set contained some spurious elevation values which were generally associated with the extension of structures into water bodies and minor discontinuities associated with some swathe edges.

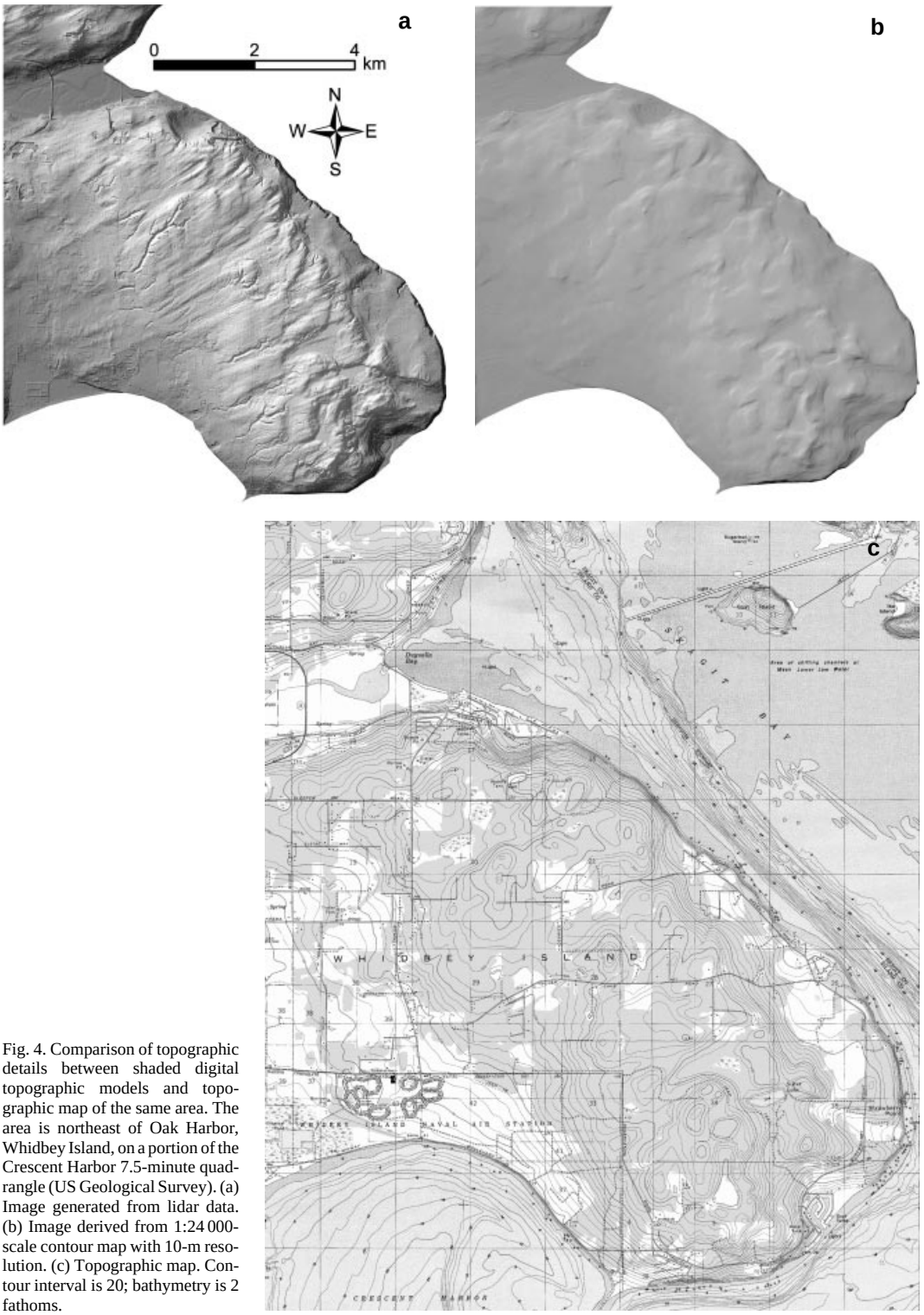

Fig. 4. Comparison of topographic details between shaded digital topographic models and topographic map of the same area. The area is northeast of Oak Harbor, Whidbey Island, on a portion of the Crescent Harbor 7.5-minute quadrangle (US Geological Survey). (a) Image generated from lidar data. (b) Image derived from 1:24 000-scale contour map with 10-m resolution. (c) Topographic map. Contour interval is 20; bathymetry is 2 fathoms.

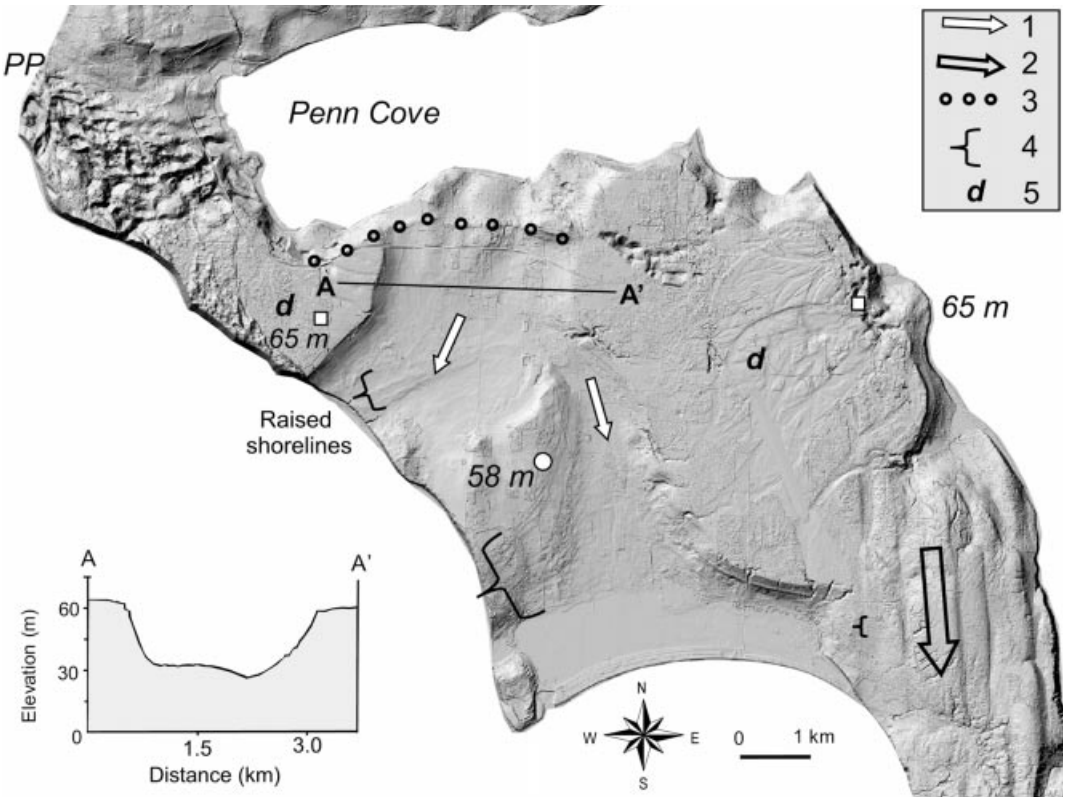

Fig. 5. Shaded digital topographic model of the Penn Cove area showing the major geomorphic features. 1 – paleochannel; 2 – inferred ice-flow direction; 3 – position of ice lobe during deglaciation; 4 – relict shorelines; 5 – raised delta surfaces; PP – Partridge Point. Refer to Fig. 2 for location.

The lidar data have the following properties: Coordinate system – State plane, Washington North zone (or HARN datum); vertical datum – North American Vertical Datum of 1988 (NAVD88); horizontal datum – North American Datum of 1983 (NAD83), 1991 adjustment; spheroid – GRS1980. Figure 4 shows a comparison between the topography represented by digital terrain modelling and a 1:24 000-scale topographic map.

Indicators of sea level

Sea level indicators in this area include, terraces, notches (erosional), beaches, deltas, bars, spits, depositional sequences, isolation basins (depositional), marine shell deposits (biological), and channels that terminate at sea level. In this study we utilize the highest local altitude of these features (mean value of several measurements) taken from the lidar data to estimate the marine limit. Ideally, sea level indicators should be assigned to specific water planes independent of their present altitude because of the uncertainty in the depth of the overlying water column at the time of deposition. In our case, we do not view this as a serious issue for the following reasons: (i) deglaciation was rapid due to the development of calving embayments in the southern Puget Sound and Strait of Georgia; (ii) sea level rise was sufficiently slow that the marine limit is defined by a single horizontal plane; (iii) our height information comes from closely spaced data points; and (iv) the vertical accuracy mentioned above is more precise than our efforts to tie features to benchmark locations through static survey and GPS levelling techniques. Therefore, the vertical errors associated with our estimates (± 2 m) are de-

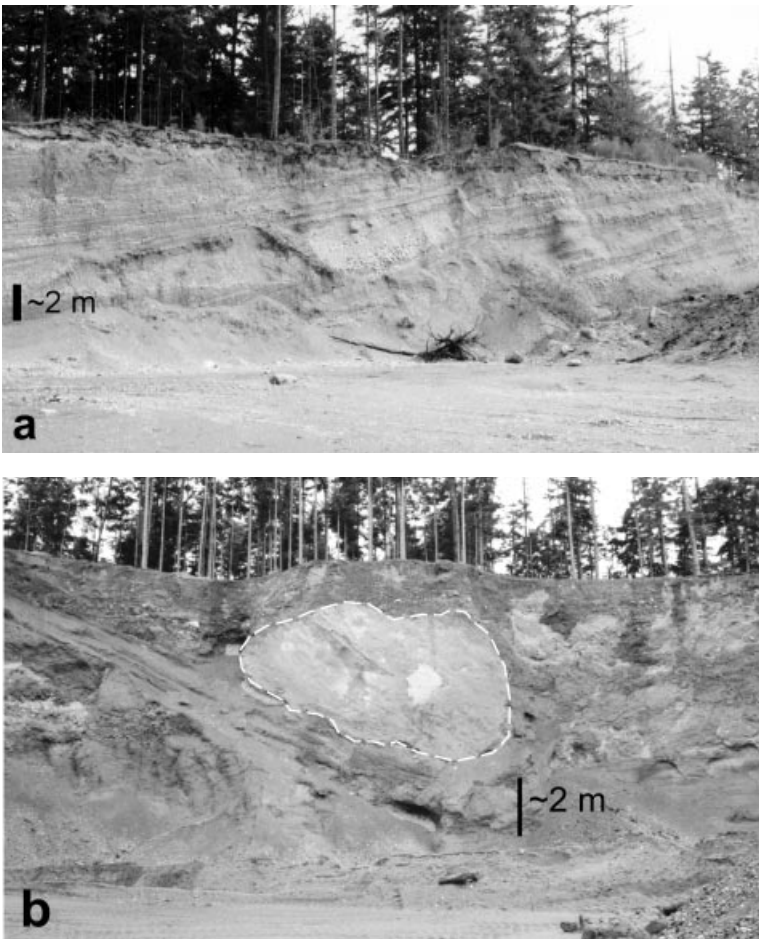

Fig. 6. (a) Photograph of an exposure showing southwestward-dipping deltaic deposits in north wall of a gravel pit north of Oak Harbor. Orientation of exposure is N280°; dip is up to 15°. Five other gravel pits in the area display similar features. (b) Photograph of an exposure showing large clast of stony mud (outlined by white dashed line) in south wall of a gravel pit north of Oak Harbor.

pendent on several factors including the height/amplitude of the sea level indicator, and our measurements of these features based on the lidar data.

The Everson glaciomarine and marine sediments include (1) fossil-bearing, stony silt, sand, matrix-supported, diamicton containing, till-like mixtures, and (2) marine clay, deltaic sand and gravel, fluvial clay, silt, and gravel that were rapidly deposited in a marine environment (Armstrong and Brown 1954; Easterbrook 1963, 1968; Domack 1983, 1984). Dethier *et al.* (1995) provided a generalized description of these sediments and grouped them into several overlapping zones that extend from beneath ice to tens of kilometers from the ice margin. These include ice-proximal, transitional, distal, marine and estuarine, and emergence facies which were used to guide their interpretations of Everson-age glaciomarine deposits.

Ice flow data

We have inferred the direction of ice movement from the orientation of drumlins and lineations. A length/width ratio ranging from 3 to >10 can be found in this region. Fabric measurements in the stony mud have not been conducted at this stage of the inquiry.

Radiocarbon age estimates

Radiocarbon ages from the glaciomarine deposits define the lower age limit of marine inundation throughout the area. These include old scintillation dates and new atomic mass spectrometer (AMS) dates. The radiocarbon ages were converted to sidereal time (2-sigma age range) using the calibration program CALIB REV 4.4, which applies the

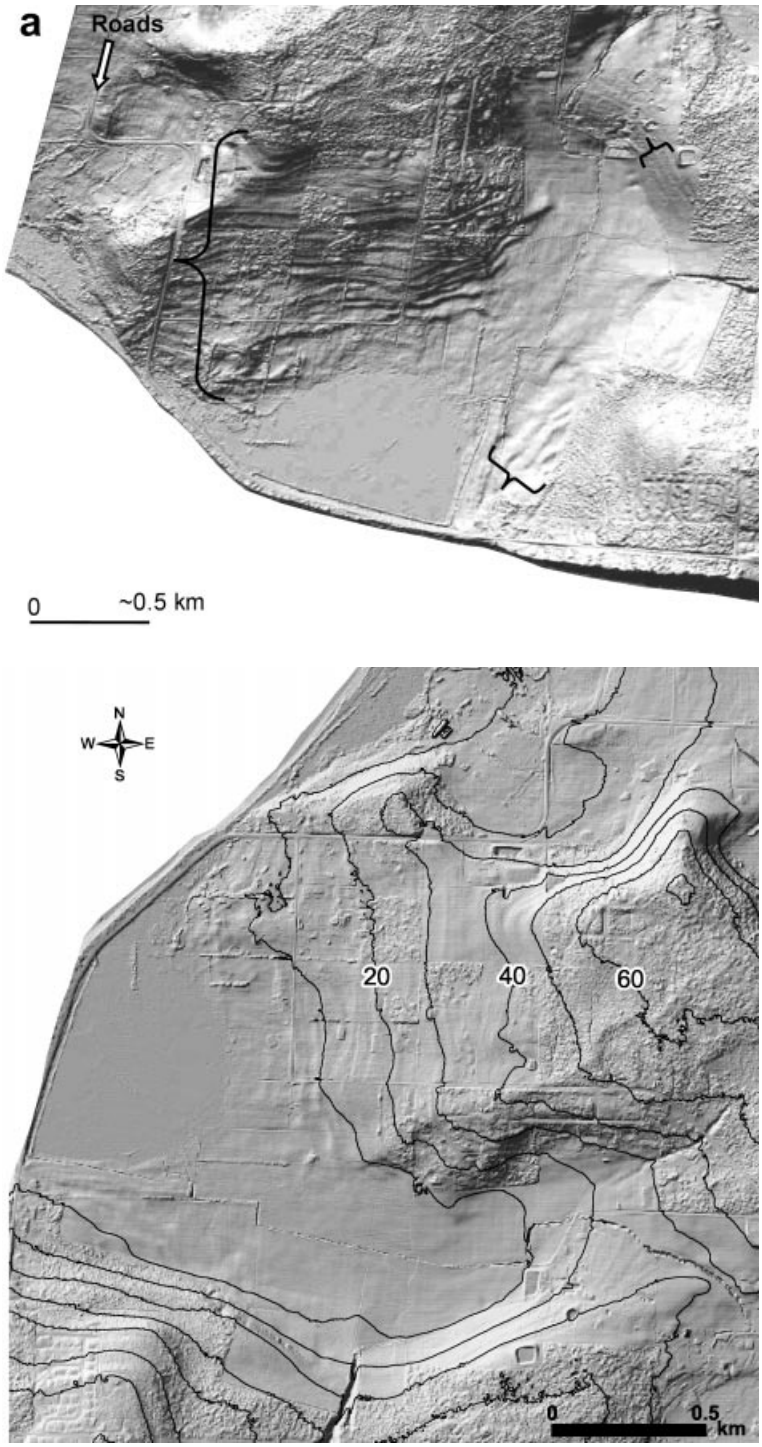

Fig. 7. (a) Shaded digital topographic model showing raised shoreline sequences northwest of Oak Harbor, Whidbey Island. Image is shown at an oblique viewing angle toward the east to better visualize the raised shorelines. Lower image is the map view of the same area. Note the difference between the topographic expression of the roads and the raised shorelines. (b) Shaded digital topographic model showing relic shorelines around Livingston Bay, Camano Island. Image is shown at an oblique viewing angle toward the northeast to better visualize the raised shorelines. Scale varies on images with oblique viewing angle. Contour interval on images in map view is 10 m.

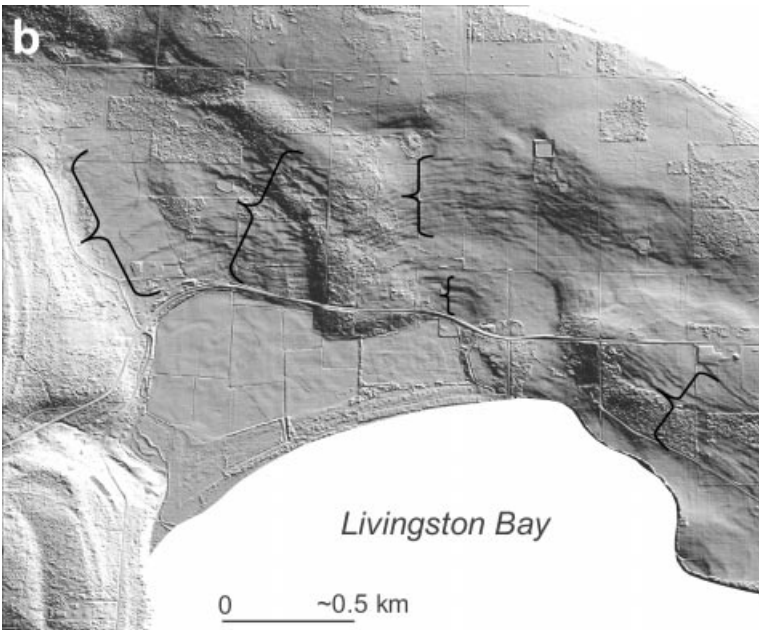

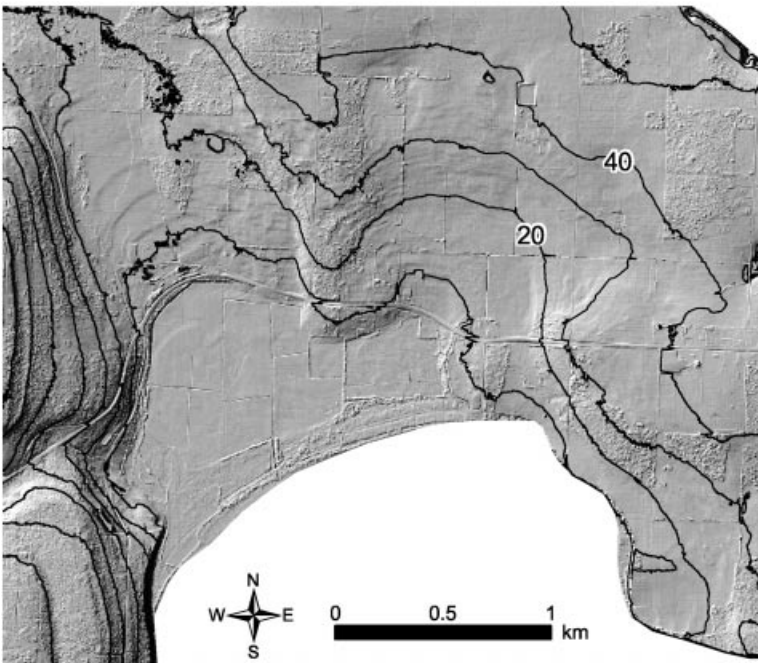

Fig. 7 Continued

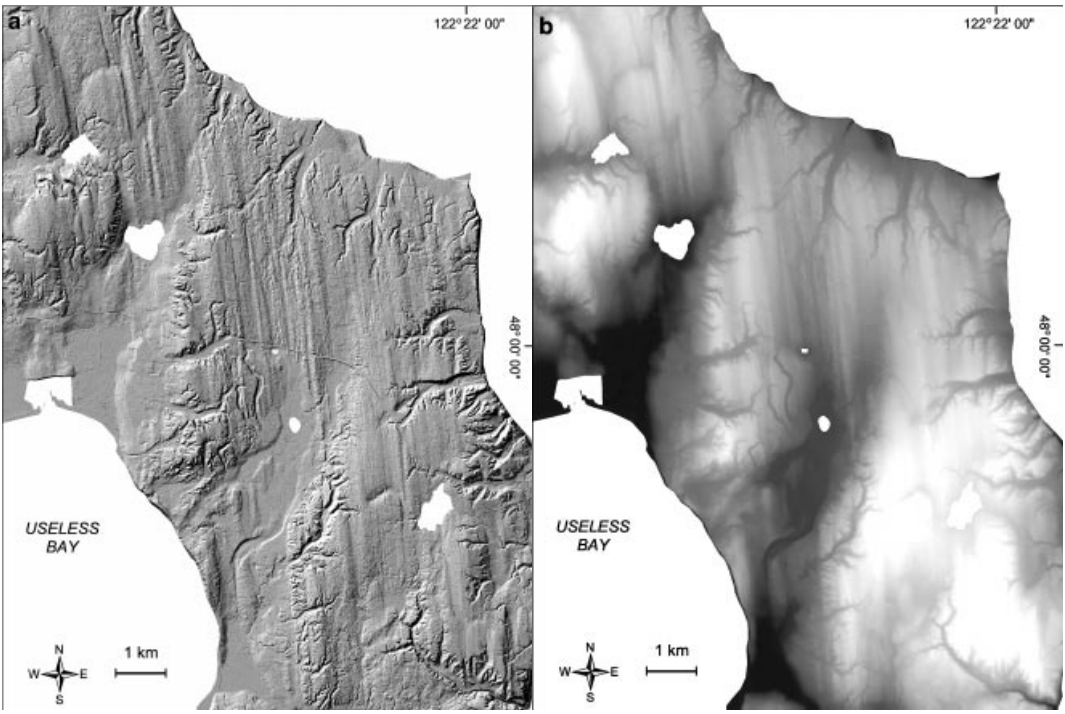

Fig. 8. (a) Shaded digital topographic model of southern Whidbey Island from lidar data showing channels graded to a higher sea level. (b) Topographic context of channels in *a*. Light areas are topographically high; refer to Fig. 2 for location.

1998 international calibration datasets (Stuiver and Reimer 1993; Stuiver *et al.* 1998). Marine shell ages were corrected using a total marine reservoir value of –800 ± 25 years (Robinson and Thompson 1981).

Results from Whidbey and Camano Islands

Altitude of sea level indicators associated with deglaciation

The lidar images reveal evidence of sea level indicators scattered between present day sea level up to *c.* 90 m (Fig. 2). An example of a large prograding delta is shown in Fig. 5 and records the *maximum* altitude of the marine limit. The surface of the delta shows distributary channels and appears unaffected by wave action, suggesting that uplift at that time was greater than eustatic sea level rise. A well defined tidewater ice margin also exists along the south and west sides of Penn Cove and suggests that marginal retreat during deglaciation was in the form of a receding local ice lobe that covered at least the central and northern portions of Whidbey Island (Easterbrook 1968, 1969; Domack 1983, 1984; Carlstad 1992). Elsewhere (northern Whidbey Island) deltaic sequences grade upward into a muddy diamicton (Fig. 6). Generally, the diamicton is texturally highly variable and there are no consistent lateral facies associations. The capping diamicton often contains large blocks of remobilized diamicton (till?), and therefore were probably built or deposited directly against receding ice (synglacial). These deposits are consistent with those mapped by Domack (1983) as ice-marginal sediment flow, proximal meltwater fan, and turbidite channel. The radiocarbon dates mentioned above come from this diamicton and show no systematic geographic trends, so we cannot say if the deltas are older farther to the south (diachronic).

Raised marine shoreline sequences were preserved best in low-sloping paleo-inlets and record the *minimum* altitude of the marine limit. Some of these shorelines are cut into the stony mud drape and form subtle wave-cut terraces. Others lap onto the muddy diamicton, consist of a thin sandy, gravel lag and may be up to 2 m high. Representative

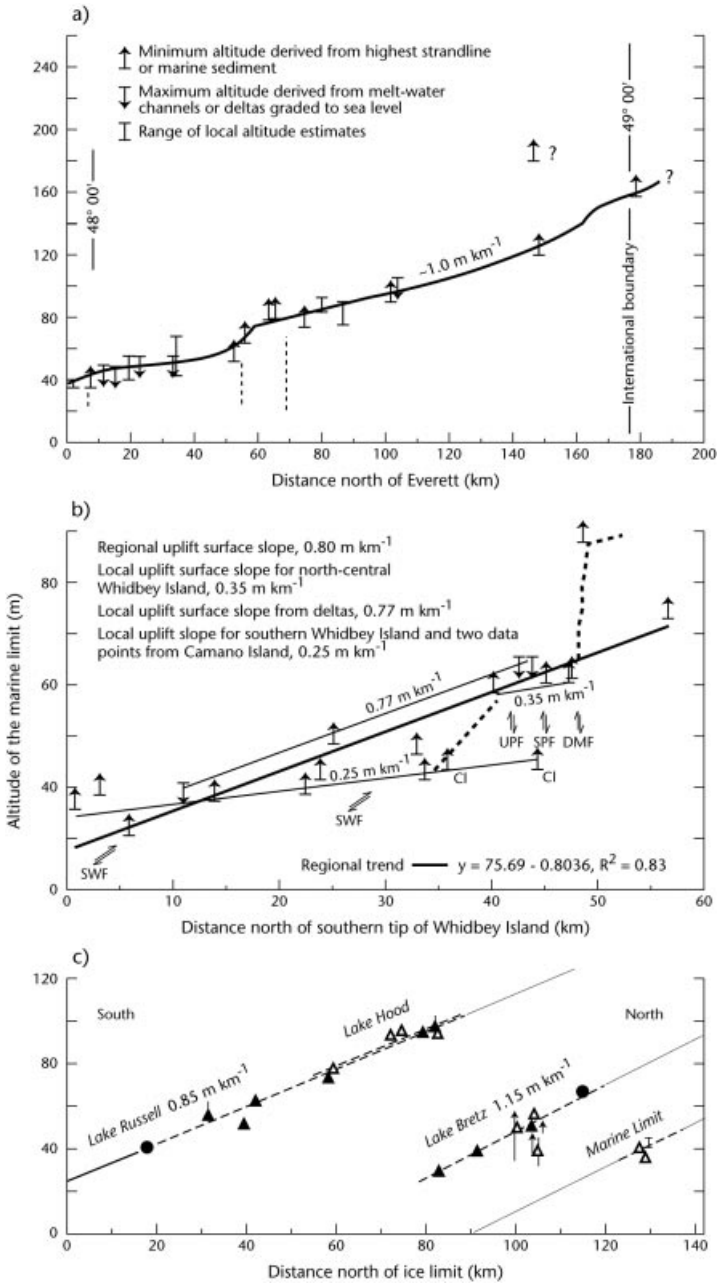

Fig. 9. North-south profiles of features associated with the marine limit. (a) Maximum altitude of the marine limit along 122°15' 00" from near Everett to the international boundary (adapted from Dethier *et al.* 1995; their Fig. 7). Data are from within 20 km of the transect. Dashed lines represent the intersection of bedrock structures. (b) Profiles of features associated with the marine limit on Whidbey and Camano islands. Data are from Fig. 2 projected onto roughly a N10° W transect. All data points are within 10 km of the transect. The postglacial uplift surface trend is derived from linear regression analysis and notation is after Dethier *et al.* Arrows show sense of relative movement of Quaternary faults. Dashed lines indicate departures from the local regression line that may or may not be associated with vertical displacement along the complex fault zones. The southern Whidbey Island fault zone intersects the N-Stransect at an oblique angle. (c) Profile of features associated with glacial lakes Russell, Hood, Bretz and the marine limit (after Thorson 1989; his Fig. 5). Some data points are projected from the eastern Puget Sound area. Refer to Fig. 1 for the location of transects.

shoreline sequences are shown in Fig. 7. The shorelines have not yet been directly dated, but must postdate the muddy diamicton and are younger than the southwest-northeast ice flow indicators on northern Whidbey Island (discussed below). We do not know if the emergence episodes have been accomplished through intermittent uplift (coseismic?) or rapid emergence, and/or a combination of these processes. On steeper coastlines the sea level indicator consists predominantly of the recognition of depositional sequences sometimes associated with ice marginal deltas and the overlying glaciomarine sediments and channels graded to the height of the sea level plane (see Dethier *et al.* 1995).

In some areas on the upland of southern Whidbey Island small channels dissect the linear elements and drumlins (Fig. 8). The channels are graded to the altitude of the local sea level. We envision that the formation of the upland channels was limited by discharge from nearby ice during deglaciation and by falling relative sea level at that time because no other source of water exists on the island. Many more features (notches, small deltas) are present in the area; the location of those shown in Fig. 2 and plotted on Fig. 9 are the best examples. Small lakes are observed in depressions and may be relicts of either small marine inlets stranded by postglacial sea level lowering or dead ice (kettle).

Surface trend of sea level indicators from lidar data

The plots on Fig. 9 show the altitude of the marine limit on roughly a N–S transect from the southern Puget Sound to the international boundary. These represent relative sea level values since about 16 967 cal yr BP which is a maximum age estimate. Our data points were projected onto a transect (B-B´; Fig. 1) which bisects the study area and is generally parallel to the direction of ice flow during the advance of the former Puget Lobe. The profiles of Dethier *et al.* (1995; Fig. 9a) and Thorson (1989; Fig. 9c) are shown for completeness and comparison.

Data from Whidbey and Camano islands indicate a minimum postglacial uplift surface slope, with an increase to the north at about 0.76 m km^{-1} using all the available data points (Fig. 2). Locally, the slope varies from 0.25 m km^{-1} to 0.77 m km^{-1}. Excluding two data points from Camano Island because they are exceedingly low, the regional uplift surface is then 0.80 m km^{-1} (error, ± 0.09 at 95% confidence interval; $R^2 = 0.83$). The variable altitude of the local uplift surface slope could be caused if uplift was restrained by diminishing ice thickness, movement along the fault zones, and/or preferential preservation of the sea level indicators. Dethier *et al.* (1995) found that the Devils Mountain fault zone coincides with a 10-m inflection point on his plot of the maximum altitude of the marine limit and this is reproduced in our estimates. The data points however are too widely spaced to provide valid constraints for the movement of these local structures. The lower uplift slope (0.25 m km^{-1}) for north-central Whidbey may be the result of sea level lowering during ice retreat or could represent the locus of crustal depression near the margin of the ice sheet. The uplift slope for southern Whidbey (including two data points from Camano Island) from features that represent minimum estimates is also lower than the regional slope. This may be the case if these features developed during a short delay in uplift. The uplift slope (0.77 m km^{-1}) calculated from the raised deltas more closely represents the regional trend as these features represent the maximum marine limit and formed synglacially during ice retreat. Because the data, sites have not been corrected for tectonic uplift rates and were projected to a transect inferred to represent a minimum estimate of the marine limit, this may explain some of the apparent variability seen in Fig. 9. Dethier *et al.* (1995; Fig. 9a) calculated an average uplift gradient at about 0.6 m km^{-1}, steepening locally to >1.3 m km^{-1}. The average is about 1.0 m km^{-1}. Thorson (1989) calculated an average uplift gradient of 0.85 m km^{-1} (Lake Russell) and 1.15 m km^{-1} (western Lake Bretz) for relict proglacial lake shorelines to the south.

Global post-glacial sea level curves are characterized by two brief periods of sea level acceleration (i.e. meltwater pulse, MWP) superimposed on a continuous rise of sea level. These two meltwater pulses, MWP-1A (*c.* 20 m, *c.* 16 000–12 500 cal yr BP) and MWP-1B (*c.* 25 m, *c.* 11 500–9 000 cal yr BP) are thought to correspond to massive inputs to freshwater derived from melting continental ice (e.g. Fairbanks 1989; Bard *et al.* 1990; Lambeck *et al.* 2002). In this area, the timing of the sea level changes is constrained between about 15 960–12 364 cal yr BP and therefore overlaps the age range for MWP-1A. Along with other considerations, such as ^{14}C plateaus in the calibration curve, make construction of isostatic uplift rates problematical. Nevertheless, Dethier *et al.* (1995)

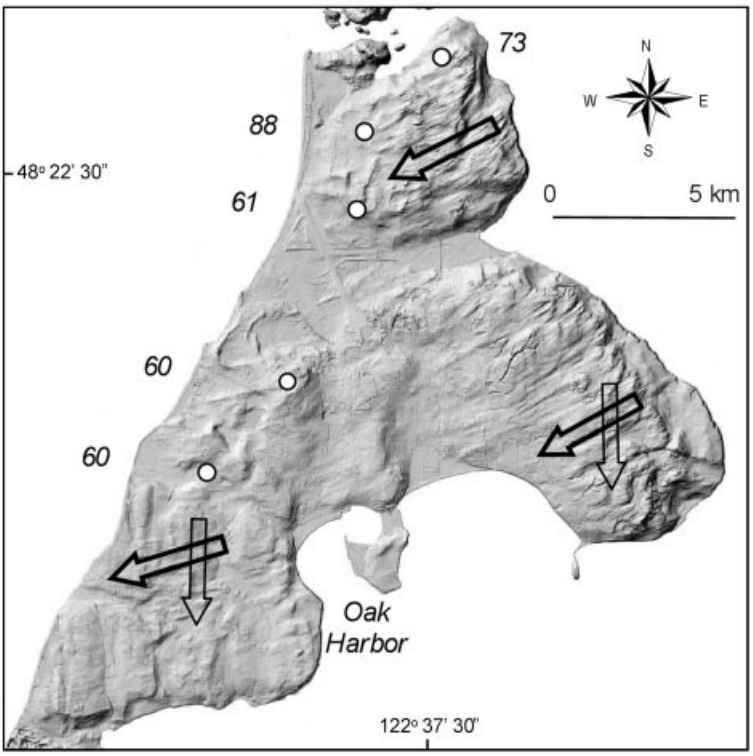

Fig. 10. Shaded digital topographic model of northern Whidbey Island showing two directions of ice-flow.

calculated rebound rates of >0.1 to 0.05 m a^{-1}, which seemed to indicate that emergence occurred before about 11 300 ^{14}C yr BP. We note, however, that his shell ages were not corrected using a marine reservoir correction and therefore the crustal rebound rates may be overestimated. Once the radiocarbon ages have been corrected, the ages seem to roughly agree within the observational errors. Clearly, only with accurate and precise dating of these and other features associated with the marine limit, along with precise altitude control, can we improve our understanding of the rebound rates, and the spatial and temporal pattern of sea level change in this area.

Direction of ice flow

For all of Camano Island and most of Whidbey Island, a single north-south flow pattern is indicated by the orientation of bedforms (drumlins and flutes, lineations; Figs. 2, 10). However, on northern Whidbey Island a NE-SW orientation of flow is indicated by superimposition of lineated topography, and is therefore somewhat younger in age. The change in ice flow direction has been noted by other researchers (Thorson 1980; Dethier 2000), but not to this extent. Thorson attribute this to retreat of the ice front in the Strait of Juan de Fuca that preceded retreat of ice in the Puget Sound, inducing a local change in the flow direction. Much of the surficial material in this area has been mapped as a blanket of glaciomarine sediments (Easterbrook 1963; Pessl *et al.* 1989). Based on these observations, clearly the deposition processes are much more complicated, likely involving glaciomarine and marine processes, combined with remolding of sediments at the ice/bed interface and meltout along the ice margin which at times may have been either floating (i.e. tidewater margin) or pinned on the topography.

The significance of this divergent ice flow direction is probably linked to the mode of deglaciation. The main questions that arise are (i) does the change in ice flow direction represent two distinct ice flow events and/or a change in flow configuration as the ice sheet thinned during deglaciation

(e.g. Thorson 1980); and (ii) what are the glacio-isostatic effects? These questions involve aspects of the rates of melting of the land-based ice, and the ice volumes and thickness when the ice became buoyant. During deglaciation once the ice had thinned to a critical level (or sea level rose to a level where ice floated), the formation of large floating ice shelves between the Juan de Fuca Strait and grounded ice on Whidbey Island resulted. The breakup or collapse of a large portion of the (floating) ice is supported by the many radiocarbon dates (141) that define the narrow time range of glaciomarine deposition in the region (e.g. Easterbrook 1992, 2003). The distribution of dates seems to indicate that deposition of the glaciomarine deposits was fairly contemporaneous and very rapid over the study region and persisted until about 11 500 ^{14}C yr BP. Following what may be inferred as a collapse of at least the marine based portion of the Puget Lobe, new pinning points were likely established in land-based areas. Several basal peat dates from abandoned meltwater channels *c.* 70 km to the northeast (the direction of ice retreat) are 11 413 ± 75 and 11 080 ± 100 ^{14}C yr BP (Kovanen 2002; Kovanen and Easterbrook 2002b) indicating that ice retreat was very rapid.

Discussion

High-resolution lidar data and digital terrain modelling reveal new information on changes in sea level and ice flow direction in the northern Puget Lowland. The altitude/amplitude of the high-stands appear to vary with latitude due to (i) differences of the ice load during deglaciation; (ii) the process of isostatic uplift; (iii) differing rheological characteristics; and (iv) possibly tectonic activity. Ages on uplifted shoreline sequences and deltas are not well constrained. In fact, no dates have been reported on any of the shoreline sequences or deltas shown here. Therefore it is difficult to examine the relative contributions of global (eustatic), regional (glacio-isostatic) and local (tectonics and sedimentary) processes with regard to the rebound rate.

These high-resolution images generated from lidar data combined with detailed field observations offer an opportunity to eventually construct detailed sea level curves that reflect components of eustatic, isostatic, and tectonic processes, all of which operate on different spatial and temporal scales. The degree of variability in the timing of the maximum postglacial marine limit is not well constrained. Correlating sea level indicators from Whidbey Island with those on the mainland to the north (e.g. Siegfried 1978; Easterbrook 1992) or on Vancouver Island (James *et al.* 2002) is difficult without detailed radiocarbon control, but this opens future prospects of constructing more detailed regional sea level curves. A comparison of our height information is generally consistent with the maximum marine limit of Dethier *et al.* (1995). Because much of our data provide minimum estimates, some northern Whidbey Island data fall up to 20 m below the inferred marine limit. Altitude differences probably reflect the fact that we have taken the highest recognizable shoreline and/or delta to represent the local marine limit; the Dethier *et al.* limit is extrapolate from sites to the east on the mainland.

Conclusions

The main contribution of this paper is the recognition of raised postglacial sea level indicators from high-resolution lidar on Whidbey and Camano islands. Our ability to incorporate the lidar data in our studies improves the visibility of subtle features, enhances our interpretations of earth surface processes at different time scales and because of this may provide alternatives to evaluate. The regional tilt of the postglacial uplift surface of 0.80 m km^{-1}, with local variability from 0.25 m km^{-1} to 0.77 m km^{-1}. The range in variability probably reflects development of features during restrained postglacial uplift, tectonic deformation, and preferential preservation/location of features in sheltered areas. The range of values reported here are slightly lower than those reported for estimates from proglacial lake shorelines (Thorson 1989) south of our study area, and consistent with those for estimates from glaciomarine and marine sediments (Dethier *et al.* 1995), adjacent to and north of our study area.

Acknowledgements

We thank the Puget Sound Lidar Consortium (especially J. Harless and D. Martinez) for providing the lidar data and kind assistance. Eric Leinberger is also thanked for drafting Figs 1 and 9. Comments from S. Porter, D. Easterbrook, D. Dethier, R. Hebda on an early draft of this paper are appreciated. Two anonymous referees provided constructive criticisms, which helped to improve and clarify the manuscript.

Dori Kovanen, Department of Geography, University of British Columbia, 1984 West Mall, Vancouver, British Columbia, V6T 1Z2, Canada.
E-mail: dkovanen@geog.ubc.ca

Olav Slaymaker, Department of Geography, University of British Columbia, 1984 West Mall, Vancouver, British Columbia, V6T 1Z2, Canada.
E-mail: olav@geog.ubc.ca

References

Anundsen, K., Abella, S., Leopold, E., Stuiver, M. and Turner, S., 1994: Late-glacial and early Holocene sea level fluctuations in the central Puget Lowland, Washington, inferred from lake sediments. *Quaternary Research,* 442: 149–161.

Armstrong, J.E., 1981: Post-Vashon Wisconsin glaciation, Fraser Lowland, British Columbia. *Geological Survey of Canada Bulletin,* 34 pp. 322.

Armstrong, J.E. and Brown, W.L., 1954: Late Wisconsin marine drift and associated sediments of the lower Fraser Valley, British Columbia, Canada. *Geological Society of America Bulletin,* 65: 349–364.

Armstrong, J.E., Crandell, D.R., Easterbrook, D.J. and Noble, J.B., 1965: Late Pleistocene stratigraphy and chronology in southwestern British Columbia and northwestern Washington. *Geological Society of America Bulletin,* 76: 321–330.

Baltsavias, E.P., 1999: Airborne laser scanning: basic relations and formulas. *ISPRS J. of Photogrammetry and Remote Sensing,* 54: 199–214.

Bard, E., Hamelin, B., Fairbanks, R.G. and Zindler, A., 1990: Calibration of the ^{14}C timescale over the past 30 000 years using mass spectrometric U-Th ages from Barbados corals. *Nature,* 345: 405–410.

Berger, G.W. and Easterbrook, D.J., 1993: Thermoluminesence dating tests for lacustrine, glaciomarine, and floodplain sediments from western Washington and British Columbia. *Canadian Journal of Earth Sciences,* 30: 1815–1828.

Blunt, D.J., Easterbrook, D.J. and Rutter, N.W., 1987. Chronology of Pleistocene sediments in the Puget Lowland, Washington. *Washington State Department of Natural Resources, Division of Geology and Earth Resources Bulletin,* 77: 321–353.

Booth, D.B., 1994: Glaciofluvial infilling and scour of the Puget Lowland, Washington, during ice-sheet glaciation. *Geological Society of America Geology,* 22: 695–698.

Carlstad, C.A., 1992: Late Pleistocene deglaciation history at Point Partridge, central Whidbey Island, Washington. Ms. Thesis. Western Washington University.

Clague, J., Harper, J.R., Hebda, R.J. and Howes, D.E., 1982: Late Quaternary sea levels and crustal movements, coastal British Columbia. *Canadian Journal of Earth Sciences,* 19: 567–618.

Dethier, D.P., Pessl, F., Jr., Keuler, R.F., Balzarini, M.A. and Pevear, D.R., 1995: Late Wisconsinan glaciomarine deposition and isostatic rebound, northern Puget Lowland, Washington. *Geological Society of America Bulletin,* 107: 1288–1303.

Dethier, D.P., 2000: Chronology and divergent flow directions during latest Pleistocene ice retreat, northeastern Puget lowland. *Geological Society of America Abstracts with Programs,* 32, A10.

Domack, E.W., 1983: Facies of late Pleistocene glacial-marine sediments on Whidbey Island, Washington: An isostatic glacial-marine sequence. *In:* Molnia, B.F. (ed.). Glacial-Marine Sedimentation. Plenum, New York, 535–570.

Domack, E.W., 1984: Rhythmically bedded glaciomarine sediments on Whidbey Island, Washington. *Journal of Sedimentary Petrology,* 54: 589–602.

Dyke, A.S. and Peltier, W.R., 2000: Forms, response times and variability of relative sea level curves, glaciated North America. *Geomorphology,* 32: 315–333.

Easterbrook, D.J., 1963: Late Pleistocene glacial events and relative sea level changes in the northern Puget Lowland, Washington. *Geological Society of America Bulletin* 74: 1465–1483.

Easterbrook, D.J., 1968: Pleistocene stratigraphy of Island County, Washington. *Washington Department of Water Resources Water Supply Bulletin* 25. 34 pp.

Easterbrook, D.J., 1969: Pleistocene chronology of the Puget Lowland and San Juan Islands, Washington. *Geological Society of America Bulletin,* 80: 2273–2286.

Easterbrook, D.J., 1992: Advance and retreat ot the Cordilleran Ice Sheets, USA. *Gèographie Physique et Quaternaire,* 46: 51–68.

Easterbrook, D.J., 1979: The last glaciation of northwest Washington. *In:* Society of Economic Paleontologist and Mineralogists (SEPM) Symposium Volume, Tulsa, Oklahoma, 177–189.

Easterbrook, D.J., 1992: Advance and retreat of the Cordilleran Ice Sheets, USA. *Géographie Physique et Quaternaire,* 46: 51–68.

Easterbrook, D.J., 1994: Chronology of pre-late Wisconsin Pleistocene sediments in the Puget Lowland, Washington. *In*: R Lasmanis and E.S. Cheney (eds): Regional Geology of Washington State: Washington Division of Geology and Earth Resources Bulletin 80, 191–206.

Easterbrook, D.J., 2003: Comment on the paper 'Determination of ^{36}Cl Production Rates from the Well-Dated Deglaciation Surfaces of Whidbey and Fidalgo Islands, Washington' by T. W. Swanson and M.C. Caffee. *Quaternary Research,* 59: 132–134.

Fairbanks, R.G., 1989: A 17 000-year glacio-eustatic sea level record: Influence of glacial melting rates on Younger Dryas event and deep-ocean circulation. *Nature,* 342: 637–642.

Haugerud, R.A., Harding, D.J., Johnson, S.Y., Harless, J.L. and Weaver, C.S., 2003: High-resolution lidar topography of the Puget Lowland, Washington – a bonanza for earth science. *Geological Society of America Today,* June: 4–10.

Heusser, C.J., 1973: Environmental sequence following the Fraser advance of the Juan de Fuca lobe, Washington. *Quaternary Research,* 3: 284–306.

Hewitt, A.T. and Mosher, D.C., 2001: Late Quaternary stratigraphy and seafloor geology of eastern Juan de Fuca Strait, British Columbia and Washington. *Marine Geology,* 177: 295–316.

James, T.S., Hutchinson, I. and Clague, J., 2002: Improved relative sea level histories for Victoria and Vancouver, British Columbia, from isolation-basin coring. *Geological Survey of Canada, Current Research,* 2002-A16, 7 p.

Johnson, S.Y., Dadisman, S.V., Mosher, D.C., Blakely, R.J. and Childs, J.R., 2002: Active tectonics of the Devils Mountain fault and related structures, northern Puget Lowland and eastern Strait of Juan de Fuca Region, Pacific Northwest. U.S. Geolgocial Survey Professional Paper, 1643, 45 p.

Johnson, S.Y., Potter, C.J., Armentrout, J.M., Miller, J.J., Finn, C. and Weaver, C.S., 1996: The southern Whidbey Island fault, an active structure in the Puget Lowland, Washington. *Geological Society of America Bulletin,* 108: 334–354 and oversize insert.

Kelsey, H.M., Sherrod, B., Johnson S.Y. and Dadisman, S.V., 2004: Land-level changes from a late Holocene earthquake in

the northern Puget Lowland, Washington. *Geology*, 32: 469–472.

Kovanen, D.J., 2002: Morphologic and stratigraphic evidence for Allerød and Younger Dryas age glacier fluctuations of the Cordilleran Ice Sheet, British Columbia, Canada and Northwestern Washington, U.S.A. Boreas, 31: 163–184.

Kovanen, D.J., 2003: Sea level changes, isostatic movements, and ice-flow indicators on Whidbey and Camano Islands, northern Puget Lowland: geologic data from LIDAR-aided observations. *In:* D.J. Easterbrook, D.J. (ed.): Quaternary Geology of the United States INQUA 2003 Field Guide Volume, 268–270.

Kovanen, D.J. and Easterbrook, D.J., 2002a: Paleodeviations of radiocarbon marine reservoir values for the NE Pacific. *Geology*, 30: 243–246.

Kovanen, D.J. and Easterbrook, D.J., 2002b: Extent and timing of Allerød and Younger Dryas age (*c.* 12.5–10.0 ^{14}C kyr BP) oscillations of the Cordilleran Ice Sheet in the Fraser Lowland, Western North America. *Quaternary Research*, 57: 208–224.

Kovanen, D.J. and Slaymaker, O., 2003: Lake Terrell upland glacial resurgences and implications for late-glacial history, Northwestern Washington State, U.S.A. *Canadian Journal of Earth Sciences*, 40: 1767–1772.

Lambeck, K., Yokoyama, Y. and Purcell, T., 2002: Into and out of the Last Glacial Maximum: sea level change during Oxygen Isotope Stages 3 and 2. *Quaternary Science Reviews*, 21: 343–360.

Mathews, W.H., Fyles, J G. and Nasmith, H.W., 1970: Postglacial crustal movements in southwestern British Columbia and adjacent Washington State. *Canadian Journal of Earth Sciences*, 7: 690–702.

Pessl, F. Jr., Dethier, D.P., Booth, D.B. and Minard, J.P., 1989: Surficial geologic map of the Port Townsend 30- by 60-minute quadrangle, Puget Sound region, Washington. U.S. Geological Survey Miscellaneous Investigations Series, Map I–1198-F, scale 1:100 000, with 13 p.

Porter, S.C and Swanson, T.W., 1998: Radiocarbon age constraints on rates of advance and retreat of the Puget Lobe of the Cordilleran Ice Sheet during the last glaciation. *Quaternary Research*, 50: 205–213.

Puget Sound Lidar Consortium, 2002: http://rocky2.ess.washington.edu/data/raster/lidar/index.htm.

Western Regional Climate Center 2003: *http://www.wrcc.dri.edu*.

Robinson, S.W. and Thompson, G., 1981: Radiocarbon corrections for marine shells dates with application to southern Pacific Northwest Coast pre-history. *Syesis*, 14: 45–57.

Siegfried, R.T., 1978: Stratigraphy and chronology of raised marine terraces, Bay View Ridge, Skagit County, Washington. Ms. Thesis. Western Washington University.

Stuiver, M. and Reimer, P.J., 1993: Extended 14C data base and revised CALIB 3.0 14C age calibration programme. *Radiocarbon*, 35: 215–230.

Stuiver, M., Reimer, P.J., Bard, E., Beck, J.W., Burr, G.S., Hughen, K.A., Kromer, B., McCormac, F.G., v.d. Plicht, J. and Spurk, M., 1998: INTCAL98 Radiocarbon age calibration 24 000 – 0 cal BP. *Radiocarbon*, 40: 1041–1083.

Swanson, T.W. and Caffee, M.L., 2001: Determination of ^{36}Cl production rates derived from the well-dated deglaciation surfaces of Whidbey and Fidalgo Islands, Washington. *Quaternary Research*, 56: 366–382.

Thorson, R.M., 1980: Ice-sheet glaciation of the Puget lowland, Washington, during the Vashon State (late Pleistocene). *Quaternary Research*, 13: 303–321.

Thorson, R.M., 1989: Glacio-isostatic response of the Puget Sound area, Washington. *Geological Society of America Bulletin*, 101: 1163–1174.

Thorson, R.M., 1996: Earthquake recurrence and glacial loading in western Washington. *Geological Society of America Bulletin*, 108: 1182–1191.

Wehr, A. and Lohr, U., 1999: Airborne laser scanning – AN INTRODUCTION AND OVERVIEW. *ISPRS Journal of Photogrammetry and Remote Sensing*, 17: 68–82.

Manuscript received March 2004, revised and accepted October 2004.